Identification and *in vivo* validation of a 9-mer peptide derived from FSHβ with FSHR antagonist activity

Kaushiki S. Prabhudesai[1], Sahil Raje[1], Ankita Dhamanaskar[1], Deepak Modi[2], Vikas Dighe[3], Alessandro Contini[4],Susan Idicula-Thomas[1]*

[1]Biomedical Informatics Centre, ICMR-National Institute for Research in Reproductive Health, Mumbai 400012, Maharashtra, India

[2]Department of Molecular and Cellular Biology, ICMR-National Institute for Research in Reproductive Health, JM Street, Parel, Mumbai 400012, Maharashtra,India

[3]National Center for Preclinical Reproductive and Genetic Toxicology, ICMR-National Institute for Research in Reproductive Health, Mumbai 400012, Maharashtra, India

[4]Dipartimento di Scienze Farmaceutiche − Sezione di Chimica Generale e Organica "Alessandro Marchesini", Università degli Studi di Milano, Via Venezian, 21, 20133 Milano, Italy

*To whom correspondence should be addressed. Tel: Phone: +91 22 24192107; Fax: +91 22 24139412; Email: thomass@nirrh.res.in

Abstract:

FSH-FSHR interaction is critical for folliculogenesis as well as progression of several cancers. FSHR peptidic antagonists can circumvent the side effects associated with currently available steroidal contraceptives. The present study aims to identify the shortest peptidic stretch of FSH that can exhibit FSHR antagonistic activity. Based on homology and structural analysis of FSH-FSHR complex (PDB ID: 4AY9), a minimal continuous stretch within FSHβ seat-belt loop (FSHβ (89-97)) was identified to be crucial for FSH-FSHR interaction. Binding affinity and activity of FSHβ (89-97) peptide was evaluated using *in silico*, *in vitro* and *in vivo* methods. The peptide could significantly inhibit binding of [^{125}I] FSH to rat FSHR as well as FSH-induced cAMP production. *In vivo* administration of this peptide resulted in reduced ovarian weight in immature Holtzman female rats. The peptide inhibited transition of follicles from pre-antral to antral stage as well as progression of granulosa cells beyond G0/G1 phase. Administration of FSHβ (89-97) peptide in adult female rats inhibited conversion of testosterone to estradiol and could significantly retard folliculogenesis. In summary, FSHβ (89-97) peptide is a potential candidate for further optimization for use as fertility regulator or theranostic agent in cancer therapy.

Keywords: Follicle stimulating hormone, FSHR antagonist, Steelman-Pohley assay, MD simulation

Introduction:

Follicle stimulating hormone (FSH) and luteinizing hormone (LH) are gonadotropins secreted by anterior pituitary gland that play a critical role in reproductive health. These are heterodimeric glycoproteins composed of a common α subunit non-covalently associated with hormone specific β subunit. FSH interacts with its cognate receptor (FSHR) which belongs to the highly conserved G-protein coupled receptor (GPCR) family (1). FSHR is localized on the surface of granulosa cells in ovaries (2) and Sertoli cells in testes (3). LH interacts specifically with its receptor (LHR) expressed on surface of theca cell in ovaries (4) and Leydig cells in testes (5). The contribution of LHR to antral stage progression of follicles has not been documented. LHR expression on granulosa cells has been observed in early antral follicles and the expression increases as the follicle matures. LHR expression is found to be more in mural granulosa cells as compared to cumulus granulosa cells (6)(7)(8). In gonads, FSH-FSHR interaction predominantly activates cAMP pathway. Activated FSHR can mediate several downstream signaling pathways such as PI3K, ERK/MAPK and β-arrestin pathways depending on the target cell (9)(10).

In female reproduction, FSH is responsible for folliculogenesis, mainly through follicle selection, and steroidogenesis (11)(12). In granulosa cells of mature follicles, FSH-FSHR interaction induces aromatase expression leading to estradiol production, while LH-LHR interaction leads to progesterone synthesis (13)(14). Estradiol and progesterone helps to maintain normal reproductive cycle in females (15)(16). Exogenous FSH is routinely used to induce superovulation in assisted reproductive technology (ART) and as a corollary, FSHR antagonists have been proposed for use in contraception (17)(18). Mice knockout for FSH or FSHR are infertile due to ovarian failure suggesting its central role in regulation of female fertility (19)(20)(21)(22).

Beyond reproduction, FSHR activation by FSH is an important determinant in cancer and tumor progression. FSHR has been detected on the surface of vascular endothelial cells of many reproductive as well as non-reproductive solid tumors. FSHR expression has been reported in ovary, prostate and thyroid cancer cells (23)(24)(25). Around 50-70% of ovarian cancer tissues are known to express FSHR(26).

Considering the importance of FSH-FSHR interaction in reproduction and cancer progression, FSHR antagonists have potential therapeutic applications as contraceptives and for cancer therapy. Currently, the contraceptives available for use are steroid based preparations of estrogen and progesterone and therefore have several side-effects such as weight gain, nausea, development of venous thrombosis and breast cancer (27)(28)(29). Contraceptives of non-steroidal origin and specific to FSHR will have fewer side effects as compared to the existing ones. Several FSHR small molecule modulators have been developed in recent years. Although FSHR small molecule modulators have shown promising results *in vitro* and *in vivo*, these molecules failed to show desirable results in human clinical trials (18)(30)(31)(32).

In case of the current regimen for cancer therapy, non-specific distribution of the drug is the primary cause of observed side-effects (33). The overexpression of FSHR on cancer cells can be exploited to develop targeted therapy. Chemotherapeutic drugs conjugated to molecules that specifically bind to FSHR will mainly be accessible to the FSHR-expressing tumors thereby reducing non-specific biodistribution and elevating the cytotoxicity response (26)(34)(35).

Previously, our group had predicted, by sequence analysis and structural bioinformatics methods, the important residues in the seat belt loop of FSHβ that can influence receptor binding (36). In the present study, we have evaluated the FSHR antagonistic activity of ^{89}SDSTDCTVR^{97} (FSHβ (89-97)) peptide by a combination of *in silico*, *in vitro* and *in vivo* methods and found that the peptide behaves as a FSHR antagonist. The binding affinity and antagonistic activity of this peptide was evaluated using *in vitro* assays such as radio receptor assay (RRA) and cAMP assay. We further validated the effect of peptide on FSH-FSHR interaction in immature and adult female rats. The results collated from various *in silico*, *in vitro* and *in vivo* assays point to the fact that FSHβ (89-97) peptide has potential for therapeutic applications as FSHR modulator.

Material and Methods:

Molecular Modelling:

Preparation of receptor structure:

The model of FSHR was prepared starting from the crystal structure of FSHR bound to FSH described in the 4AY9 PDB file (37) [DOI: 10.1073/PNAS.1206643109], using the software MOE [Molecular Operating Environment (MOE), version 2015.10 Chemical Computing Group Inc.: 1010 Sherbooke St. West, Suite No. 910, Montreal, QC, H3A 2R7, Canada), 2015]. FSHR was derived from chain X (residues C18-T270), while FSH consisted of chains A and B of 4AY9.pdb (FSHα and FSHβ, respectively). Since a truncated sequence was used, FSHR was capped at both the N- and C-termini by acetyl and methylamino groups, respectively. Similarly, FSHα was capped at the N-terminus, since its sequence at the C-terminus was complete, while FSHβ was capped at the C-terminus only. The complex was then protonated at physiological pH (pH=7) by using the Protonate 3D tool of MOE and energy minimized by using the Amber10EHT force field and the Born solvation model implemented in MOE. The system was then subjected to MD simulation in explicit TIP3P water(38) at constant temperature (300 K) and pressure (1 atm.), corresponding to the Isothermal–isobaric ensemble NPT, using the *pmemd.cuda* module (39) included in the Amber18 package(40). A 1.6 ns equilibration phase, followed by 10 ns of production were conducted by following a protocol described in detail previously (41). The root mean squared displacement (RMSD) vs time was monitored for all backbone atoms to assess the stability of the complex (Fig S1). Since the RMSD profile was rapidly converged, it was not deemed necessary to go on with the simulation further. The coordinates of the last frame of the MD trajectory were converted to PDB format,

water and ions were removed, and the protein complex was energy minimized with MOE using the same protocol as above. FSH was deleted and the resulting FSHR structure was used for docking using the FlexPepDock software (42) distributed within the Rosetta 3.11 modelling package (43).

Preparation of peptide model:

The starting FSHβ (89-97) peptide was obtained from the FSHR-FSH complex model obtained as described above, by deleting all FSH residues except for the nonapeptide comprised by S89 and R97 of FSHβ. The complex between FSHR and FSHβ (89-97) peptide occupying the same site as observed within the full FSH, hereafter referred as FSHR-FSHβ (89-97)X, was used as the starting geometry for FlexPepDock. Indeed, it has been reported that FlexPepDock succeeded in driving tested peptides to their native binding conformation when starting close to the binding site (44).

Peptide docking:

Ab-initio peptide docking was performed according to the protocol described in (44). A library of trimer and pentamer peptide fragments (200 fragments for each category) was initially generated based on sequence similarity to the peptide and on the secondary structure predicted for the peptide by PSIPRED (45). Then, a prepacking stage was accomplished to the receptor in order to remove all possible side-chain clashes, accordingly to the energy function used by FlexPepDock. Docking was then performed using the same settings described in (44), requesting the generation of 50000 different models for each receptor. These models were then scored in terms of predicted binding affinity according to the *reweighted_sc* function implemented in FlexPepDock. It was recently reported that MM-PBSA and MM-GBSA calculations performed on energy-minimized complexes deriving from protein-peptide docking significantly improved the ability to discriminate the correct binding pose (46). The top 2500 models were then energy-minimized using the *pmemd* software of the Amber18 suite. The geometry optimization was performed up to a gradient of 0.1 kcal $mol^{-1} \cdot$ Å, using the ff14SB force field (47) and the GB-Neck2 implicit solvent model (48), a combination that resulted successful in previous works (49). MM-GBSA binding energy calculations were then performed on the minimized geometries by using the same force field and solvent combination as above and requesting an ionic strength of 150 mM.

MD simulations on docked complexes:

The lowest-energy complexes obtained from the above steps, hereafter referred as FSHR-FSHβ (89-97)D were subjected to MD simulations in explicit water using the same protocol described above. The RMSD vs time profile resulted, in both cases, sufficiently converged within 10 ns (Fig S2). As a comparison, the starting FSHR-FSHβ (89-97)X conformation was also evaluated by MD using the same protocol (Fig S3). All MD

simulations were conducted on commercial GPUs using *pmemd.cuda*, while trajectory analyses were performed with the *cpptraj* software of Amber18.

Nwat-MMGBSA analysis:

Relative binding affinities of FSHβ (89-97)D for FSHR were computed using the Nwat-MMGBSA approach (41) (50) (51), based on the inclusion of a limited number of explicit water molecules to improve the ranking capability of standard MM-PBSA/GBSA calculations(52). Accordingly, we requested the inclusion of 30 waters selected to be the closest to the peptide-protein interaction interface in every analysed frame; standard MM-GBSA calculations (Nwat = 0) were also performed for comparison. Interface residues were selected by *cpptraj* by selecting all ligand/receptor residues that are at 2.5 Å from receptor/ligand residues. As suggested in previous studies, (50) only polar residues were considered for selecting explicit water molecules to be included, as part of the receptor, in the MM-GBSA calculation. The analyses were conducted on the 10^{th} ns of the production run by selecting 100 evenly spaced out snapshots. The GB-Neck2 implicit solvent model was used for the GB calculations (48) and a 150 mM salt molar concentration in solution was set. In all calculations, entropy was neglected. MM-GBSA calculations were performed with the MMPBSA.py script included in the AmberTools18 package (53). The same analysis was also conducted on FSHR-FSHβ (89-97)X for comparison.

Chemicals and reagents:

Pituitary purified human FSH (hFSH) was purchased from Dr. Parlow (National Hormone and Pituitary Program, CA, USA). [^{125}I]NaI was procured from Board of Radiation and Isotope Technology, India. FSHβ (89-97) peptide was custom synthesized from peptide 2.0 (Chantilly, VA USA) (HPLC and MS data: Fig S4).

Radioreceptor assay (RRA):

The FSHR binding affinity of FSHβ (89-97) peptide was determined using radioreceptor assay (RRA) as described previously (54). FSH was radioiodinated using iodogen method (55). [^{125}I] FSH (200000 cpm; 30 µci/µg) in RRA buffer (pH 7.4) containing 0.3% (w/v) bovine serum albumin was used as a tracer. Membrane preparation of Human Embryonic Kidney (HEK)-293 cell line expressing rat FSHR (HEK-rFSHR) was used as a source of FSHR (54). FSHβ (89-97) peptide was incubated with membrane preparation of HEK-rFSHR at different concentrations (600 µM-9600 µM) followed by incubation with [^{125}I] FSH for 2 h at RT. The assay was terminated by addition of RRA buffer and 5% (w/v) polyethylene glycol (PEG) followed by centrifugation at 3000 rpm for 30 min at 4°C. The supernatant was decanted and radioactivity of each pellet was counted by γ counter (Wallac 1470, WIZARD, Turku, Finland). Individual assays were carried out in triplicate. RRA was also performed at the intermediate concentrations (4800 µM, 6000 µM, 7200 µM, 8400 µM and 9600 µM) using the same protocol as mentioned above. The peptide

as well as FSH were first reconstituted in sterile distilled water and later dissolved in RRA buffer to get required concentrations. The individual assays carried out using intermediate concentrations (4800 µM-9600 µM) were performed in duplicate.

cAMP assay:

The activity of FSHβ (89-97) peptide was evaluated by their ability to alter the FSH mediated cAMP production. This assay was performed on HEK-rFSHR cells followed by measurement of cyclic adenosine monophosphate (cAMP) using commercially available enzyme immunoassay (EIA) kit (Cayman Chemical Company, Ann Arbor, MI, USA) as described previously (56). In brief, twenty-four hours after plating, cells were pretreated with Dulbecco's Modified Eagle's (DMEM/F12) serum free medium (SFM) containing 1mM isobutylmethylxanthin (IBMX). Cells were later incubated with different concentrations of FSHβ (89-97) peptide for 30 min followed by incubation with hFSH (1 ng/well) for 30 min at 37˚C. The cells were lysed using 0.1M HCl and centrifuged at 1000 g for 10 min at 4 ˚C. Supernatant was diluted using EIA buffer and used to estimate cAMP levels by ELISA. cAMP levels in presence of 1 ng of hFSH and 0 ng hFSH (basal cAMP) were also calculated. The peptide as well as FSH were first reconstituted in sterile distilled water and later on dissolved in serum free- DMEM/F12 medium. Individual assays were carried out in triplicate.

Animals

In vivo assays involved in this study were performed on Holtzman female rats, bred at ICMR - National Institute for Research in Reproductive Health (ICMR-NIRRH). The animals were kept in polypropylene cages with autoclaved paddy husk for bedding and maintained at controlled temperature (23 ± 1℃) and humidity (55 ± 5%), with a 14-h light/10-h dark cycle. Animals were supplied with food and water ad libitum. The use of animals for this study was approved by the Institutional Animal Ethics committee (IAEC no: 24/15).

Treatment of animals

A) Immature female rats:

To determine the bioactivity of the FSHβ (89-97) peptide, *in vivo* Steelman-Pohley assay was carried out using immature Holtzman female rats(57). In this study the immature female rats (21-23 days old) were first subcutaneously injected with different concentrations of FSH (0 IU, 0.5 IU,1.0 IU and 1.5 IU/injection FOLICULIN; Bharat serum and vaccines limited) along with a fixed concentration of hCG (6.6 IU/injection HUCOG 2000 I.U.; Bharat serum and vaccines limited n=5/group) in the scruff of the neck twice per day for 3 consecutive days to determine the minimal effective concentration. Later the immature female rats in positive control group were injected with 0.01M PBS followed by

injection of 1.0 IU of FSH in combination with 6.6 IU hCG twice daily for 3 consecutive days (n=7). Animals injected with 0.01M PBS followed by 6.6 IU hCG injection were treated as negative control group (n=7). In the test group, the peptide reconstituted in 0.01 M PBS was injected at a concentration of 20 mg/kg BW (200 µl) followed by hCG (test I; n=8) or combined FSH and hCG injection (test II; n=8) (58).The purity of the peptide was more than 95% (HPLC data Fig S4). FSH and hCG doses were made in 0.01 M PBS. Post 72 h of first injection, animals were sacrificed. Ovaries were collected and weighed. Ovaries were further subjected to cell cycle analysis, hematoxylin and eosin (H and E) staining and gene expression analysis.

B) Adult female rats:

The effect of FSHβ (89-97) peptide was further studied on ovarian weight, hormonal profile and ovarian morphology of adult female rats (90 days old). Animals exhibiting normal 3 consecutive estrus cycles (4 or 5 days), as determined by vaginal smears, were recruited in this study. Animals were divided into two test groups (n=5/group) and respective control groups (n=5/group). In test groups I and II, animals were injected with 4 mg/kg BW and 20 mg/kg BW of peptide respectively. In test group I, a single injection of the peptide was administered on morning of diestrus day 1 (D1). In test group II, the peptide concentration (20 mg/kg BW) was divided into four doses and animals were injected on morning and evening of diestrus days 1 and 2 (D1 and D2). Control group was maintained with animals injected with vehicle (sterile injectable water). All injections were through intravenous (IV) route.

All animals were monitored for 3 cycles post treatment and sacrificed on D1 of 4th cycle by CO_2 asphyxiation and reproductive organs were harvested. For test group II, all the vital organs were also harvested and weighed to assess the effect of the higher dose of peptide. Ovaries were further stored for histopathology imaging. To study the effect of FSHβ (89-97) peptide on steroidogenesis, animals were bled on proestrus phase to estimate the serum estradiol levels and diestrus phase to estimate serum progesterone and testosterone levels of second estrous cycle post treatment (59).

***Cell cycle analysis*:**

Cell cycle analysis was performed by flow cytometry after staining the granulosa cells with propidium iodide (PI). Ovaries of sacrificed animals were collected and processed for flow cytometry as described previously(60). A total of 10,000 cells were acquired for each experiment on BD FACS Aria with argon laser (Becton Dickinson; San Diego, CA). Data were analyzed using FACS Diva Version 6.1.3 software (BD Biosciences).

Ovarian gene expression analysis:

Real time PCR was performed to study the effect of peptide on expression of aromatase, anti-mullerian hormone (AMH), inhibin A and inhibin B (Table 1).

Briefly, RNA was extracted by using TRIZOL reagent (Thermo fisher scientific). 2 µg of RNA was reverse transcribed using a commercial cDNA synthesis kit (SuperScript™ III First-Strand Synthesis System, Thermo Fisher Scientific).

Real timer PCR was carried out as detailed previously (61) using SYBR green chemistry. CFX Manager 3.1 software (Bio-Rad) was used to obtain a standard curve and generate mean threshold cycle (Ct) values for each experiment. The relative mRNA expression was calculated by ΔΔ Ct method (62). ΔCt values were calculated as the difference of the Ct values of the target gene and reference gene (18S). The difference between the control and experimental group was then obtained as ΔΔCt = [Δ Ct (experimental) - ΔCt (control)]. Quantification of the gene expression level in each sample was the mean of duplicate RT- PCR experiments.

Table 1: Sequence and annealing temperature of Primers:

Gene name	Primers	Annealing temperature (^{0}C)
18S	F: 5'-CCGCAGCTAGGAATAAT-3'	59-62
	R: 5'-AGTCGGCATCGTTTATGGTC-3'	
Aromatase	F: 5'- ACCTGGAGTAGGAGCCTTTA-3'	60
	R: 3'-GTTCAGCGGTTGGTCTGATA-5'	
AMH	F: 5'-GCTGAAGTGATATGGGAGCCT-3'	62
	R: 5'-AGGGTGGCACCTTCTTTGC-3'	
Inhibin A	F: 5'-GCACTTGAAGAAGAGACCCGAT-3'	60
	R: 5'-AATGCAGTGTCTTCCTGGC-3'	
Inhibin B	F: 5'-GCGGTGAAGAGACACATCTT-3'	62
	R: 5'-GCACCACAAATAGGTTCTGGTT-3'	

Estimation of serum estradiol, progesterone and testosterone levels:

Serum estradiol, progesterone and testosterone levels were estimated using ELISA kit (Diagnostics Biochem Canada Inc., Canada, N0L 1G2). In brief, a set of standards (range: 0 to 3200 pg/mL for estradiol and 0 to 60 ng/mL for progesterone and 0 to 16.7 ng/mL for

testosterone) and the samples were loaded into the anti-estradiol or anti-progesterone or anti-testosterone antibody coated wells for estradiol, progesterone and testosterone estimation respectively. Competition assay was set up between hormones from serum samples and antigen-HRP (Horseradish Peroxidase) conjugate. The plate was incubated on a plate shaker for 1 h at RT. 150 µL of TMB substrate was added and the reaction was allowed to take place for 15 min at RT. Reaction was terminated by adding stopping solution and plate was read at 450 nm.

Statistical analysis:

All results are presented as mean ± S.E.M. and analyzed using student's t test and ANOVA (when required). The values of *P ≤ 0.05, **P ≤ 0.01 and ***P ≤ 0.001 with respect to control group were considered as statistically significant.

Results:

Peptide docking:

To better understand the molecular basis of the interaction between FSHβ (89-97) peptide and FSHR, we performed docking calculations using the *ab-initio* docking protocol of the FlexPepDock software distributed within the Rosetta 3.11 modelling suite, as described in detail in the Method section. The top-scored poses were subjected to MD simulations to obtain a 10 ns trajectory. The last 2 ns of the MD trajectory, where the RMSD vs time profile was sufficiently converged (Fig S2), were subjected to clustering, considering the RMSD of the backbone atoms as a metric and using a protocol described in detail in a previous work(63). The representative geometries of the most populated clusters obtained by the analyses of the FSHR trajectories are depicted in Fig 1.

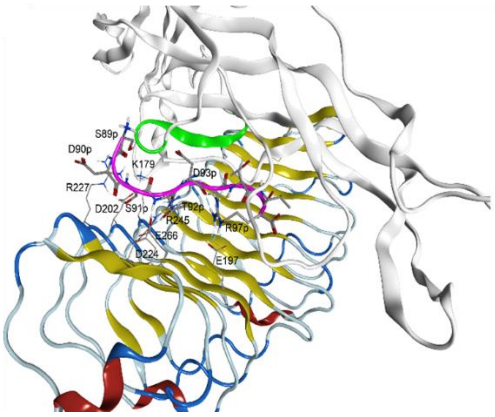

Fig 1. Predicted binding pose for FSHβ (89-97) peptide (purple) to FSHR: The ribbon representation of crystallographic FSH (light grey, with the region of FSHβ (89-97) colored in green) is also included. The Leucine Rich Repeats (LRRs) of FSHR(ECD) is represented in yellow.

It can be observed that the top pose predicted for the binding of FSHβ (89-97) (represented in purple, in Fig 1) deviates from the position occupied by the same peptide fragment belonging to the complete FSH sequence (represented in green, in Fig 1). This probably occurs because the peptide, outside its own protein environment, is not able to maintain the same conformation observed within the full FSH protein. Moreover, the binding site on FSHR is particularly flat and the binding of FSHβ (89-97) peptide can only rely on H-bonds and ionic interactions with the solvent-exposed polar residues on the receptor surface. This assumption is in concurrence with the relatively low potencies measured in *in vitro* experiments. However, several interactions can still be observed between FSHR and FSHβ (89-97) peptide (Fig 1). The peptide head triad made by S89, D90 and S91 show multiple H-bonds with R227 and D202 sidechains that are themselves joint by an ionic bond, also involving K179. Peptide T92 side chain makes a dual interaction with D224 (Thr-OH···OC(O)-D224) and R245 (Thr-O(H)···HNC(=NH2)NH-Arg) side chains. Finally, peptide R97 side chain, conformationally stabilized by an intramolecular H-bond with D93 carbonyl, makes an ionic interaction with the sidechain of E197.

Looking for a further confirmation to the above postulation, MD trajectories of FSHR complexes with docked FSHβ (89-97) were analyzed by Nwat-MMGBSA calculations. This method is a variant of MM-PBSA (52) that includes a number of explicit waters, selected to be the closest to the ligand or ligand-receptor interface and considered as part of the receptor, in the calculation(51). The method was found successful in improving computed relative binding energies for small molecule-receptor(64)(41) and protein-protein interactions(50). By looking at Table 2, it can be observed that the binding pose selected by docking is ranked above the starting pose even when MD simulatitions are performed and energy calculations are done with or without considering the role of explicit water molecules.

Table 2. Nwat-MMGBSA energies (kcal/mol)[a] computed for the starting pose and for the top-scored pose of FSHβ (89-97) docked to FSHR

Complex	Nwat=0	Nwat=30
Starting pose[b]	-9.6±0.4	-54.9±1.0
Top-scored pose[c]	-26.6±0.4	-86.5±0.9

a. Results are average MM-GBSA binding energies (kcal/mol) ± standard error of mean; the entropic contribution has been neglected. Nwat=0 corresponds to a standard MMGBSA calculation; Nwat=30 correspond to a MMGBSA calculation with 30 explicit water included at the receptor-peptide interface. b. The starting pose corresponds to the pose of the FSHβ (89-97) peptide as found in the full-length FSHβ sequence co-crystallized with FSHR. c. The top-scored pose corresponds to the highest-ranked pose obtained by docking.

Effect of FSHβ (89-97) peptide on binding of FSH and FSH induced signaling:

FSHβ (89-97) peptide was assessed to evaluate its effect on binding of [^{125}I] FSH to FSHR. FSHβ (89-97) peptide inhibited the binding of radiolabeled FSH to FSHR in dose-dependent manner. 100% binding inhibition was observed in case of highest concentration of FSHβ (89-97) peptide (9600 µM) (Fig 2A). FSHβ (89-97) peptide at intermediate concentrations from 4800µM-9600 µM showed dose dependent inhibition of FSH binding to FSHR (Fig S5).

Effect of the peptide on FSH stimulated cAMP production was evaluated in HEK-rFSHR cells pre-incubated with FSHβ (89-97) peptide. FSHβ (89-97) peptide, in a dose-dependent manner, decreased the cAMP production. At highest concentration of this peptide, FSH induced cAMP production was equivalent to basal level cAMP production (Fig 2B). Cells incubated with the peptide alone showed negligible cAMP production (data not shown).

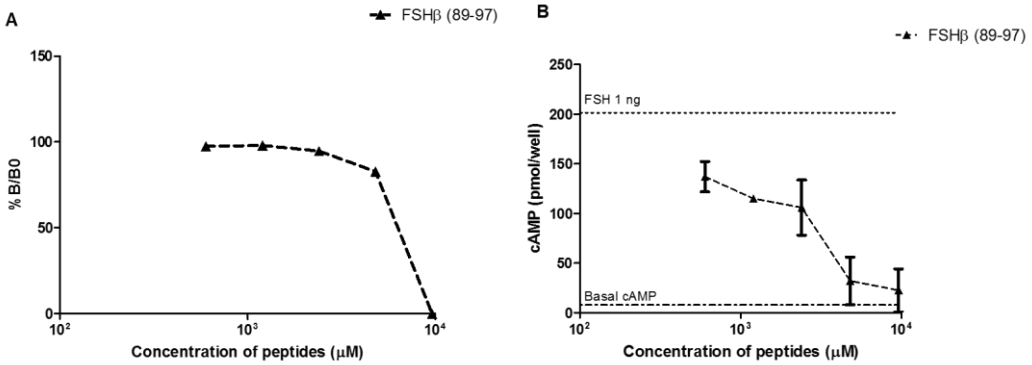

Fig 2. Effect of FSHβ (89-97) peptide on A. binding of FSH to FSHR and B. FSH-induced cAMP production: A. HEK-rFSHR cell membrane preparations were incubated with increasing concentration of FSHβ (89-97) peptide along with [^{125}I] FSH. %B/B$_0$ represents the amount of [^{125}I] FSH bound to HEK-rFSHR specifically. Nonspecific binding was determined in presence of 1 µg of FSH B. HEK-rFSHR cells were stimulated with 1 ng of hFSH in presence of different doses of FSHβ (89-97) peptide. cAMP levels measured at baseline and in response to 1 ng hFSH are indicated by dotted lines. Each point represents the mean ± SEM of a representative experiment performed in duplicates.

Effect of FSHβ (89-97) peptide on ovarian weight of immature female rats:

As compared to hCG alone, dose dependent increase in ovarian weight was observed with increasing concentrations of FSH in immature rats (Fig S6). The FSH-mediated (1.0 IU) increase in ovarian weight was abrogated when the animals were injected with the FSHβ (89-97) peptide along with FSH and hCG (Fig 3). The reduction in ovarian weight due to treatment with FSHβ (89-97) peptide was statistically significant ($p \leq 0.05$).

Administration of FSHβ (89-97) peptide along with hCG showed slight reduction in ovarian weight as compared to hCG alone.

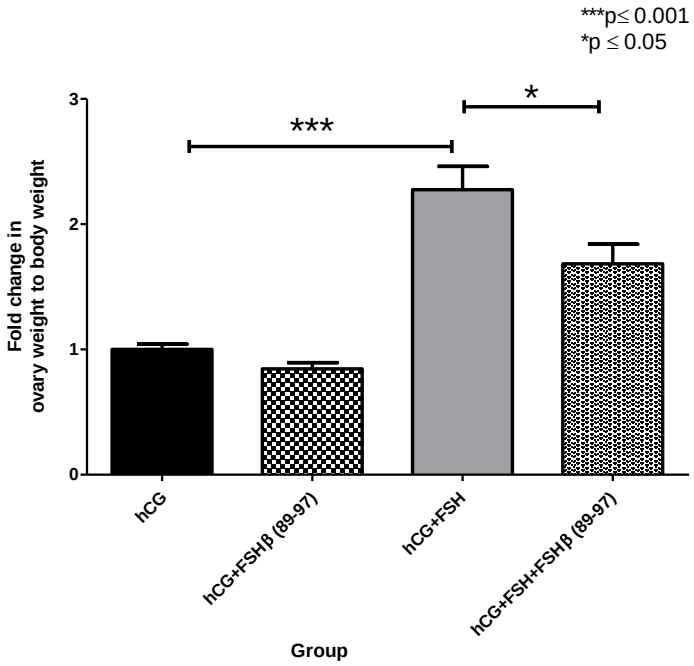

Fig 3. Effect of FSHβ (89-97) peptide on ovarian weight of immature rats: Immature female rats were injected with FSHβ (89-97) peptide (20 mg/kg BW) followed by injection of hCG alone or hCG and FSH. Parallel positive and negative controls were maintained. Post 72 h of first injection animals were sacrificed and ovarian weights were determined. Each bar and vertical line represent the mean ± SEM weight. * and *** indicate significant difference ($p \leq 0.05$ and $p \leq 0.001$ respectively).

Effect of FSHβ (89-97) peptide on FSH-mediated cell cycle progression of rat granulosa cells:

To study the effect of FSHβ (89-97) peptide on FSH mediated cell cycle progression, granulosa cells isolated from the ovaries were subjected to flow cytometry analysis. In the hCG treated animals, 90% of the cells were in G0/G1 phase and 10% of cells in S or G2/M phase. In response to FSH and hCG treatment, there was an increase in number of cells in S and G2/M phase and this increase was statistically significant as compared to hCG treated controls. The progression of cells that are actively proceeding through the cell cycle was inversely affected by treatment with FSHβ (89-97) peptide. There was a significant reduction in the number of cells in S and G2/M phase in animals treated with FSHβ (89-97) peptide along with FSH and hCG as compared to FSH + hCG group (Fig 4; Fig S7). Injection of FSHβ (89-97) peptide along with hCG however; did not show any alteration in % cell population in G0/G1, S and G2/M phase of cell cycle as compared to

hCG alone. This data suggests that the FSHβ (89-97) peptide hinders the FSH-mediated folliculogenesis in the ovary.

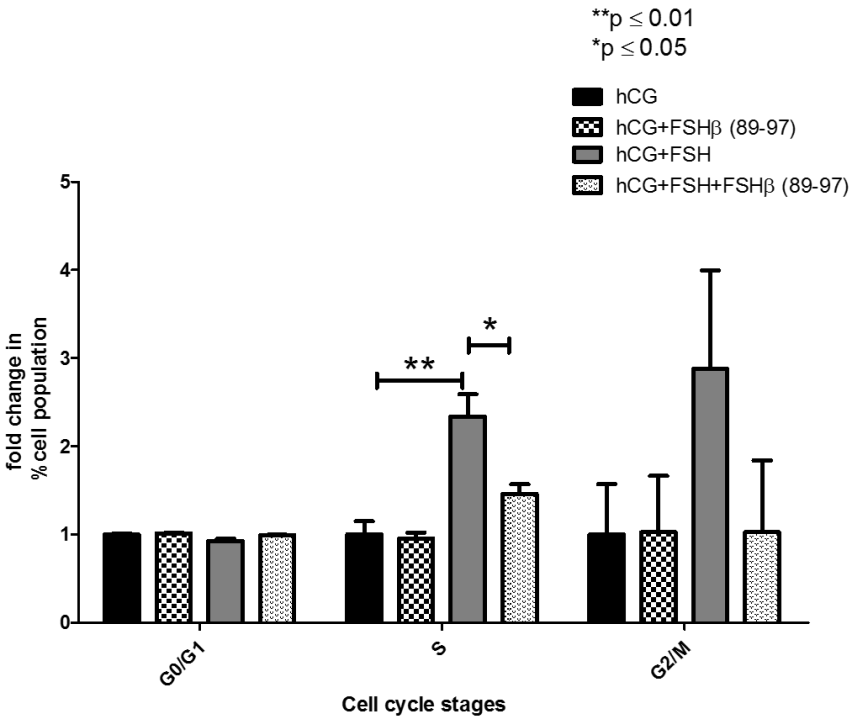

Fig 4. Effect of FSHβ (89-97) peptide on cell cycle progression in granulosa cells: Graphical representation of percentage of granulosa cell population in G0/G1, S and G2/M phase for FSHβ (89-97) peptide treated group. Each bar and vertical line represent the mean ± SEM for three independent experiments. * and ** indicate significant difference ($p \leq 0.05$ and $p \leq 0.01$ respectively).

Effect of FSHβ (89-97) peptide on ovarian morphology and folliculogenesis of immature female rats:

The cross sections of hCG-treated ovaries showed that most of the follicles were at primary and secondary stage of folliculogenesis whereas FSH and hCG treated ovaries had majority of follicles in antral stage of folliculogenesis. The cross-sections of ovaries treated with FSHβ (89-97) peptide along with FSH and hCG injection displayed more of primary, secondary and preantral follicles and fewer antral follicles as compared to FSH and hCG treatment group. The ovarian morphology of animals treated with FSHβ (89-97) peptide were similar to hCG treated animals (Fig 5).

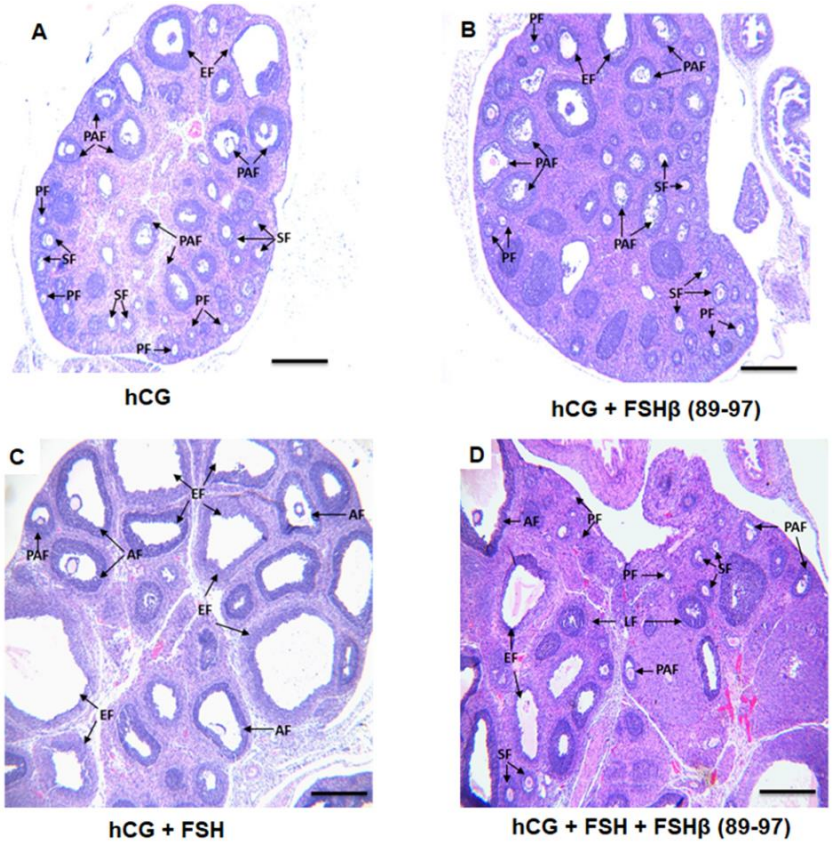

Fig 5. Effect of FSHβ (89-97) peptide on ovarian morphology: Representative images of H and E stained ovarian sections displaying primary follicles (PF), secondary follicles (SF), preantral follicles (PAF), antral follicles (AF) and empty follicles (EF) in A. hCG alone, B. hCG + FSHβ (89-97), C. hCG + FSH, and D. hCG + FSH + FSHβ (89-97). Fewer AFs and higher number of SFs and PAFs were observed in case of animals treated with FSHβ (89-97) peptide (D) as compared to FSH and hCG treatment group (C). Scale bar is equal to 200 µM.

Effect of FSHβ (89-97) peptide on ovarian gene expression:

To further understand the effect of peptide administration on folliculogenesis, gene expression analysis was performed on ovarian samples of immature female rats using real time PCR. Since administration of FSHβ (89-97) peptide along with hCG alone did not show significant alteration in ovarian weight, cell cycle progression and ovarian morphology, gene expression study was restricted to the following three groups, (i) hCG alone, (ii) hCG + FSH and (iii) hCG + FSH + FSHβ (89-97) peptide.

Animals treated with FSHβ (89-97) peptide prior to FSH and hCG injection showed reduced ovarian expression of inhibin A and aromatase genes and elevated expression of AMH, inhibin B as compared to animals treated with FSH and hCG (Fig 6). Expectedly, the expression level of aromatase was low in animals treated with hCG

alone. The data further confirms that FSHβ (89-97) inhibits FSH-FSHR interaction mediated folliculogenesis.

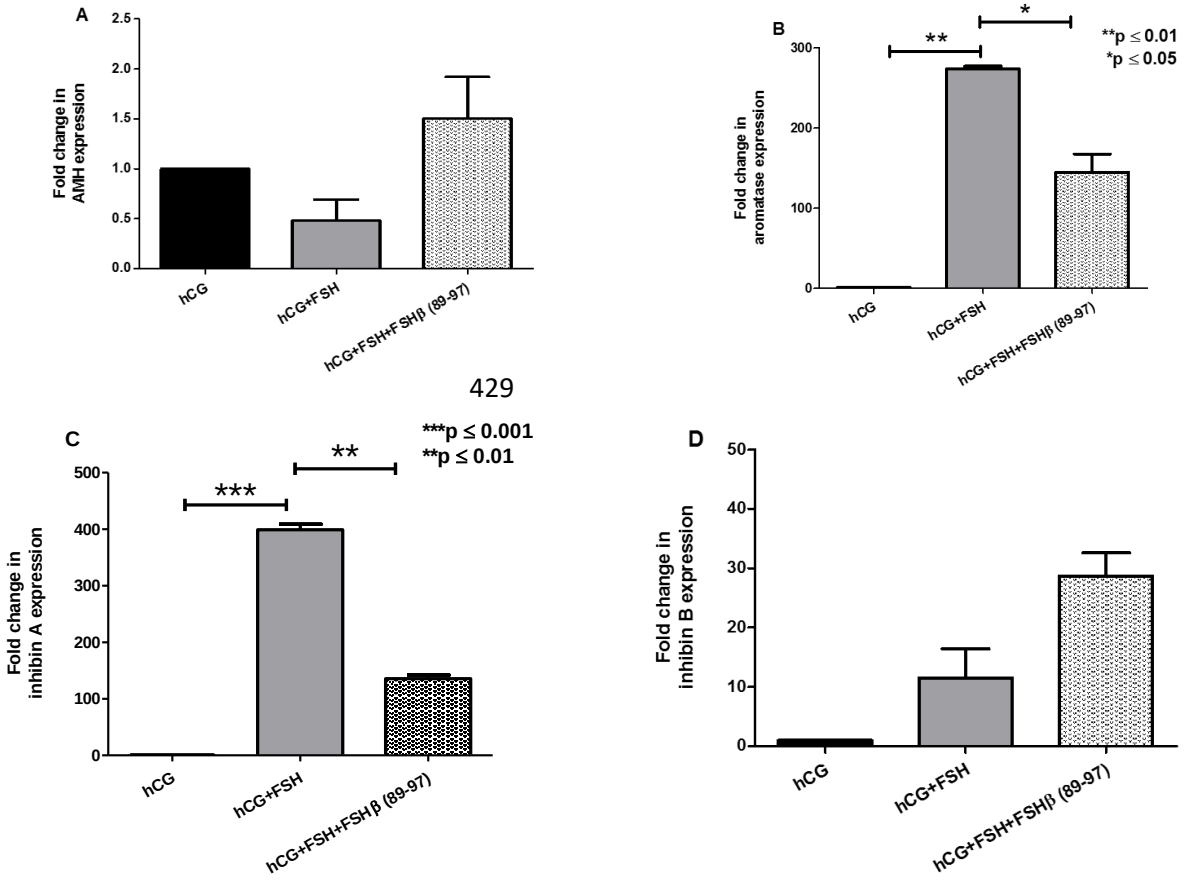

Fig 6: Effect of FSHβ (89-97) peptide on ovarian gene expression: Quantitative real time PCR was carried out on representative cDNAs of each group. Bar graphs show fold change in expression of AMH (A), aromatase (B) inhibin A (C) and inhibin B (D). *, ** and *** indicate statistically significant difference ($p \leq 0.05$, $p \leq 0.01$ and $p \leq 0.001$ respectively).

Effect of FSHβ (89-97) peptide on ovarian weight of adult female rats:

To further investigate the effect of FSHβ (89-97) peptide on the endogenous circulating FSH, adult female rats were injected with the peptide at two concentrations (4 mg/kg BW and 20 mg/kg BW). Administration of peptide at 4 mg/kg BW did not affect the ovarian weight however, at 20 mg/kg BW of peptide significant reduction in ovarian weight was observed (Fig 7B). No significant effect was observed in weight of uterus and vital organs in animals treated with higher dose of peptide (Fig S8).

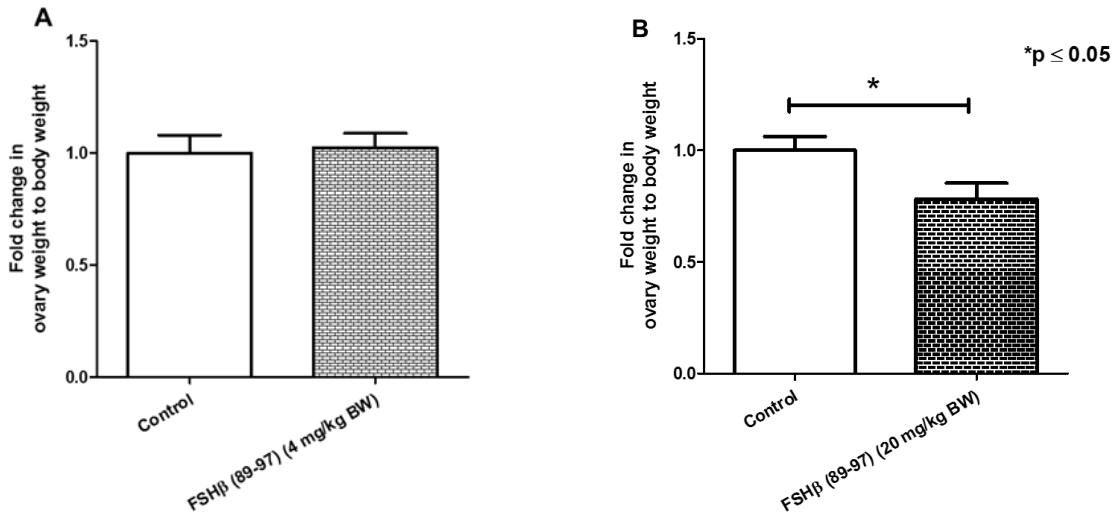

Fig 7. Effect of FSHβ (89-97) peptide on ovarian weight at diestrus phase: Adult female rats were administered with A. 4 mg/kg BW and B. 20 mg/kg BW of FSHβ (89-97) peptide. All animals were sacrificed on D1 phase of fourth estrus cycle. Each bar and vertical line represent the mean ± SEM ovarian weight. * indicates a statistically significant difference ($p \leq 0.05$) from mean of vehicle-treated control.

Effect of FSHβ (89-97) peptide on steroidogenesis in vivo:

The effect of FSHβ (89-97) peptide on steroidogenesis in adult rats was investigated by evaluating serum estradiol, progesterone and testosterone levels in control and treatment group animals. Serum estradiol levels were lower while serum progesterone and testosterone levels were elevated for peptide treated animals (4 mg/kg BW and 20 mg/kg BW) as compared to control group. Decrease in serum estradiol levels and increase in serum testosterone levels was statistically significant as compared to control group when higher dose of peptide (20mg/kg BW) was administered (Fig 8B and F).

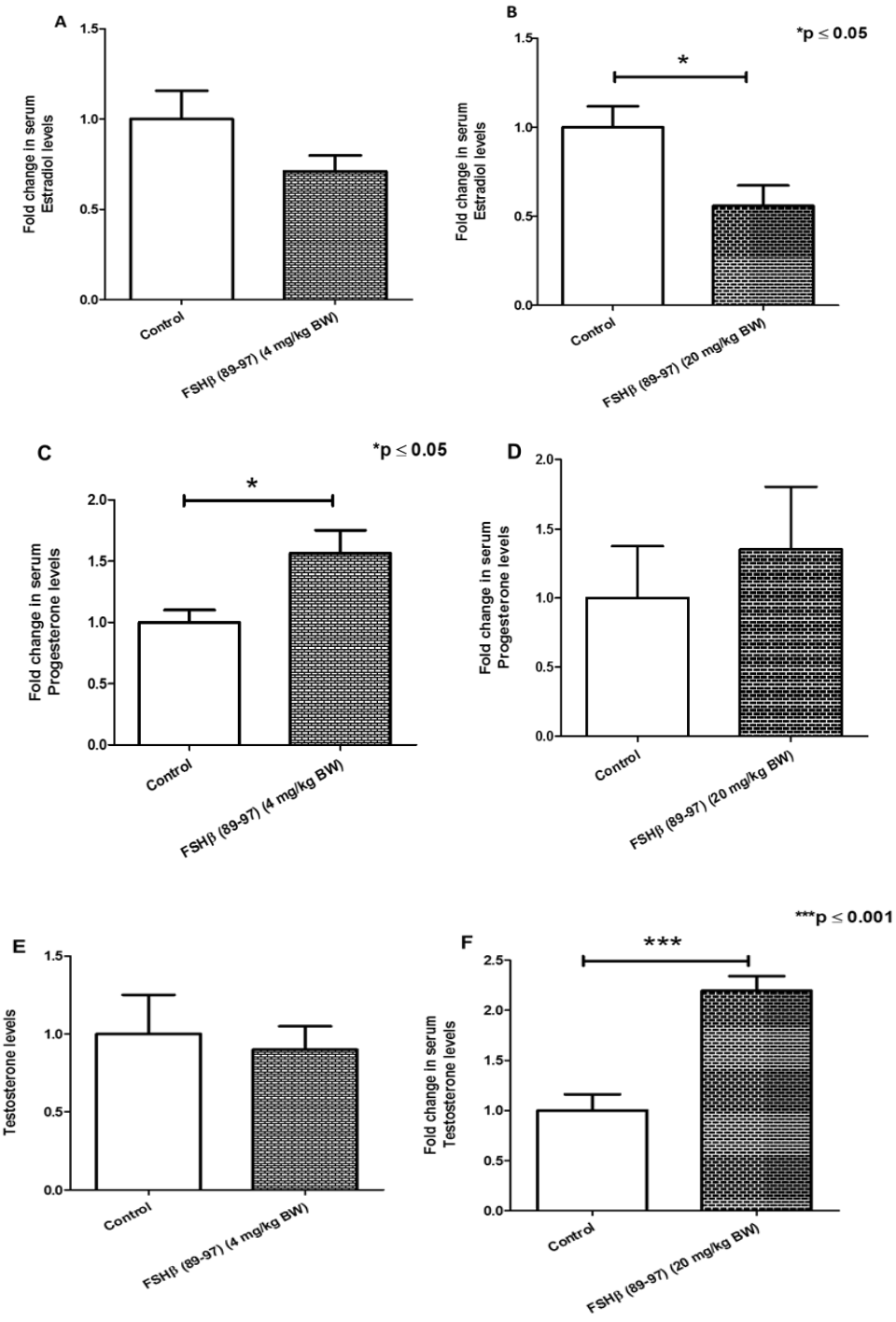

Fig 8. Effect of FSHβ (89-97) peptide on serum A-B) estradiol level at proestrus phase and C-D) progesterone and E-F) testosterone levels at diestrus phase: Adult female rats were administered with two doses of peptide (4 mg/kg BW and 20 mg/kg BW). Blood was drawn through retro-orbital bleeding at morning of proestrus and diestrus phase of second estrus cycle post treatment. Each bar and vertical line represent the mean ±SEM estradiol, progesterone or

testosterone concentration. * and *** indicate a statistically significant difference ($p \leq 0.05$ and $p \leq 0.001$ respectively) from mean of vehicle-treated control.

Effect of FSHβ (89-97) peptide on ovarian morphology and folliculogenesis of adult rats:

Ovaries collected from sacrificed animals were subjected to H and E staining to study the effect of peptide on ovarian and follicular morphology. The observations from H and E staining are focused on ovarian morphology, follicle morphology, oocyte and zona pellucida (ZP) morphology, cumulus granulosa cell morphology and theca cell morphology. Microscopic examination of ovarian tissues from treatment groups revealed atretic changes in granulosa cells and altered oocyte morphology of mainly late antral follicles. Theca cell morphology was however found to be unaltered in treatment group (Fig 9A). These alterations were found to be more significant in case of 20 mg/kg BW of peptide dose. To confirm the effect of the peptide administration (20 mg/kg BW) on follicular development, the secondary and antral stage follicles were counted and compared in control and treatment group. Although, ovarian tissues from control as well as treatment groups showed presence of empty follicles (no oocyte), its number was much higher in case of treatment group. In treatment group, the number of antral follicles was found to be significantly reduced and number of secondary follicles was higher as compared to control group indicating that the transition of follicles from secondary to antral stage, which is dependent on FSH-FSHR interaction (12), has been adversely affected due to peptide treatment (Fig 9B).

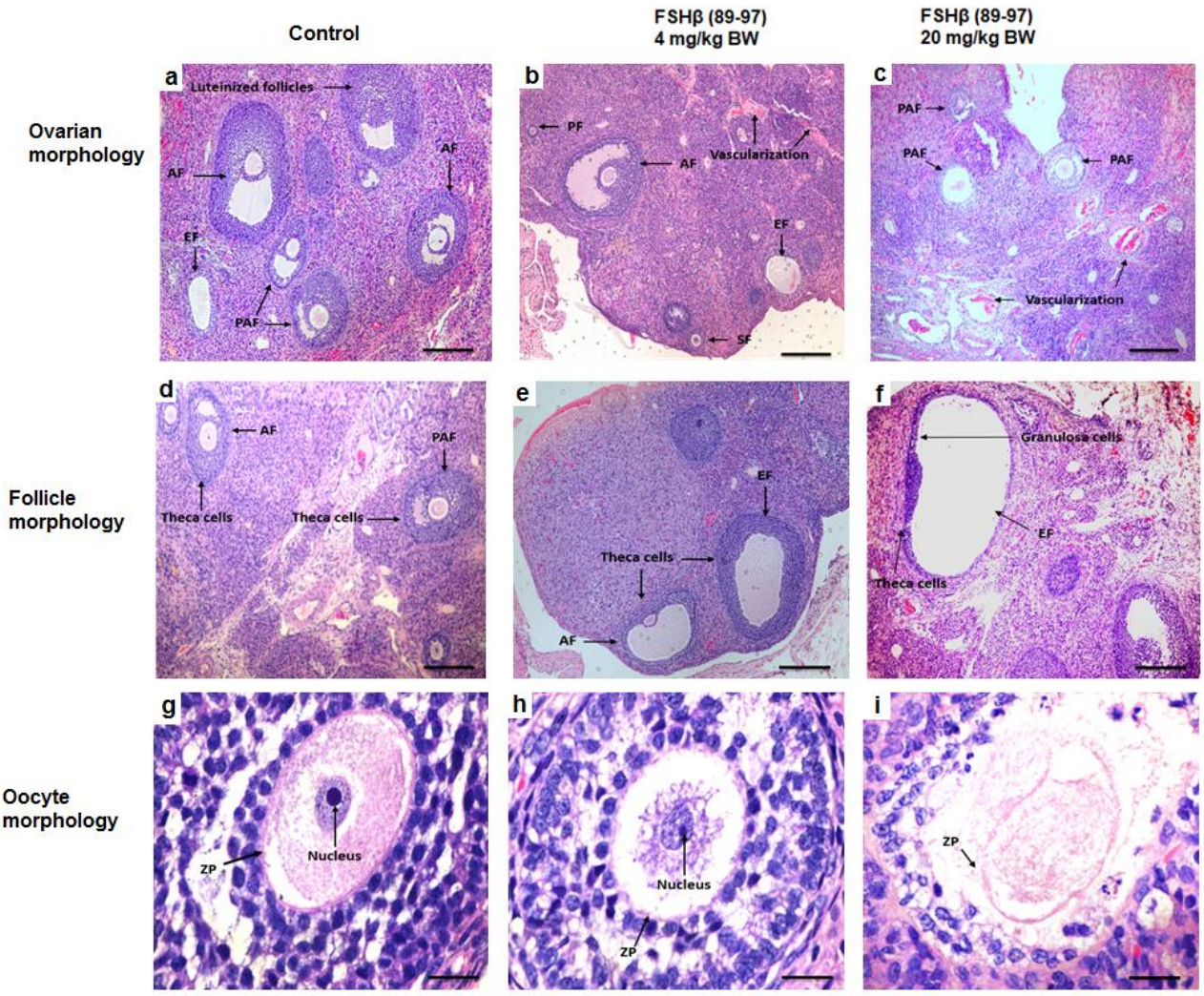
Control
FSHβ (89-97)
4 mg/kg BW
FSHβ (89-97)
20 mg/kg BW
Ovarian morphology
Follicle morphology
Oocyte morphology
a
Luteinized follicles
AF
AF
EF
PAF
b
PF
AF
Vascularization
EF
SF
c
PAF
PAF
PAF
Vascularization
d
AF
PAF
Theca cells
Theca cells
e
EF
Theca cells
AF
f
Granulosa cells
EF
Theca cells
g
Nucleus
ZP
h
Nucleus
ZP
i
ZP

486

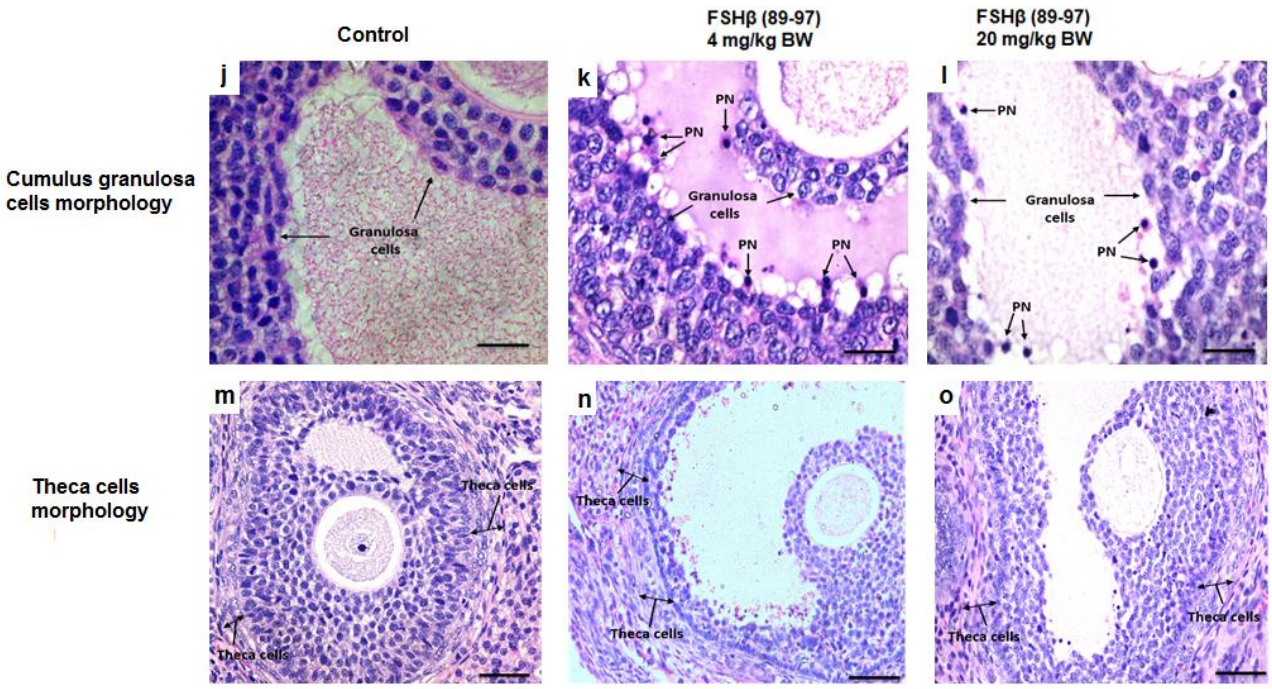

487

488 **Fig 9A. Effect of FSHβ (89-97) peptide on ovarian morphology of adult female rat:**
489 Representative micrographs of ovarian morphology (a-c), follicle morphology (d-f), oocyte
490 morphology (g-i), cumulus granulosa cells morphology (j-l) and theca cells morphology (m-o).
491 Histopathology observations showed presence of higher number of antral follicles (AF) in control
492 group as compared to treatment group. Treatment group ovaries showed higher number of
493 secondary (SF) and preantral follicles (PAF) as compared to control group (a-c). Treatment group
494 ovaries also showed increased vascularization (b and c). Large number of empty follicles was
495 observed in treatment group ovaries (d-f). Ovarian tissues of control group showed healthy oocyte
496 in antral follicles as compared to treated ovarian sections (g-i). Ovarian sections of treatment
497 group also showed presence of atretic granulosa cells and pyknotic nuclei (PN) (j-l). Morphology
498 of theca cells was found to be unaltered in control as well as the treatment groups (m-o). Scale
499 bar is equal to 200 µM.

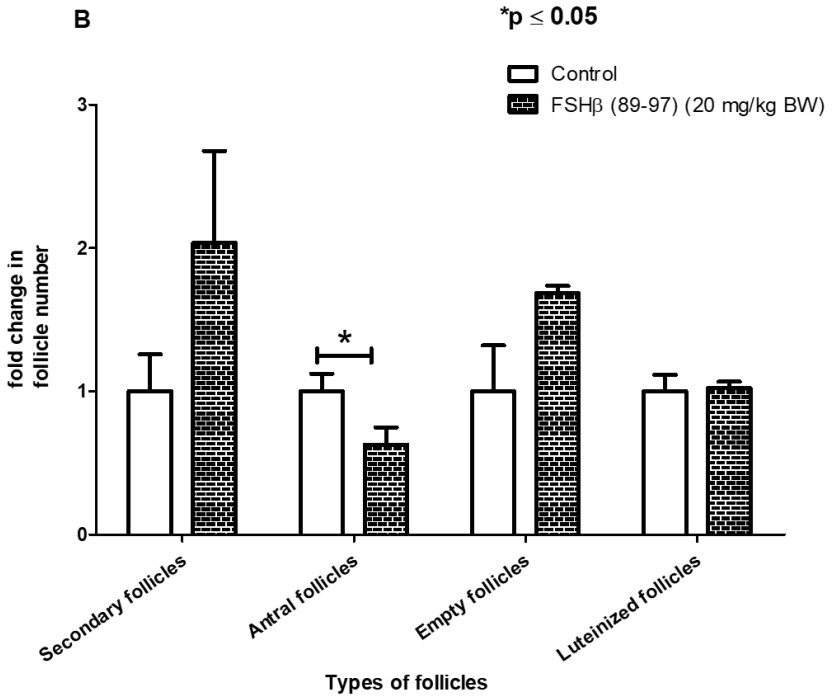

Fig 9B. Effect of FSHβ (89-97) peptide at 20 mg/kg BW on folliculogenesis: Effect of FSHβ (89-97) peptide on follicle development stages were monitored at diestrus phase. Animals sacrificed on D1 stage were subjected to histopathology imaging. Follicles at different stages of folliculogenesis (a. secondary follicles b. antral follicles c. empty follicles d. luteinized follicles) were counted. * indicates a statistically significant difference ($p \leq 0.05$) from mean of vehicle-treated control.

Discussion:

FSH-FSHR interaction plays a central role in regulation of female reproduction, mainly in ovarian function, by driving folliculogenesis and steroidogenesis (12)(13). Considering the importance of FSH-FSHR interaction in reproduction and tumor progression (24)(34), there is an increasing need to identify molecules harboring FSHR agonist or antagonist activity.

The partial crystal structure of FSH-FSHR (ECD) complex reveals that amino acids 89 to 105 of FSHβ forms a seat belt segment and interacts with leucine-rich repeat (LRR) region of FSHR (65). Prior to the elucidation of the crystal structure, these residues along with its neighboring residues (85-108) have been shown to be critical for receptor specificity by several chimeric studies involving hCG/FSHβ subunit (66) or LH/FSHβ subunit (67) or through use of hormone specific peptides (68). In an attempt to predict the residues important for binding specificity of FSH-FSHR, we had previously carried out sequence and structural analysis of bound FSH-FSHR complex(36)(37) (ECD; 4AY9). The analysis revealed that the amino acids S89, D90, T95, V96 and R97 are critical for FSHR binding (36). In the present study, to further evaluate the role of these amino acids in FSHR binding, a 9-mer peptide, FSHβ (89-97) was designed and subjected to several

rounds of docking simulations with hFSHR (ECD) in presence of FSH. Computational simulations suggested that FSHβ (89-97) peptide could bind to hFSHR (ECD) and prevent the binding of the native ligand FSH (Fig 1). Analysis of the docked complexes revealed that central residues of FSHβ (89-97) (S91, T92 and C94) do not interact with hFSHR (ECD). These observations (Fig 1) are in concurrence with our previous results obtained by sequence and structural analysis of hFSH-hFSHR (ECD) (36). The docking studies provide insight that FSHβ (89-97) peptide can bind to hFSHR (ECD) wherein the N- and C-terminal residues make critical contacts with ECD of hFSHR.

To validate the *in silico* observations and evaluate the effect of FSHβ (89-97) peptide on FSH-mediated bioactivity, we further carried out various *in vitro* assays such as RRA and cAMP assay as well as *in vivo* assays which involved monitoring ovarian weight, examination of ovarian morphology, cell cycle analysis, gene expression analysis and hormonal profiling.

We observed inhibition of [^{125}I] FSH binding to FSHR in dose dependent manner in presence of FSHβ (89-97) peptide (Fig 2A). FSH-FSHR interaction induces cAMP production as a result of adenylate cyclase activation(9). *In vitro* experiments showed that this peptide significantly blocked FSH-mediated cAMP production in a dose dependent manner (Fig 2B). Taken together, the observations from docking studies, RRA and cAMP assays indicate that a) the peptidic stretch of 89-97 amino acids is critical for FSHR binding and b) the peptide has FSHR antagonistic activity.

Subsequently, the FSHR antagonistic activity of FSHβ (89-97) peptide in *in vivo* was validated by monitoring ovarian weight of immature and adult female rats (57)(69). Steelman-Pohley assay was performed to understand the effect of peptide on ovarian weight of immature rats. In this assay, ovarian weight gain in response to exogenous FSH or FSH-like molecule in immature female rats is used as a surrogate indicator of FSH activity. We observed that exogenous administration of urofollitropin (hFSH) increased the ovarian weight of immature rats. This increase in ovarian weight was attenuated by subcutaneous administration of FSHβ (89-97) peptide (Fig 3). In adult female rats, endogenous circulating FSH stimulates development of ovaries. Females with FSH/ FSHR mutations are known to have small ovaries(70)(71)(72). When adult animals were injected with the peptide at 20 mg/ kg BW, significant reduction in ovarian weight was observed as compared to control group (Fig 7B), suggestive of the peptide having FSHR antagonistic activity both *in vitro* and *in vivo*.

Decrease in the ovarian weight which was persistent in immature as well as adult female rats may be attributed to retarded granulosa cell division and follicle maturation. To confirm this, the granulosa cells of immature rats treated with FSH with and without the peptide were analyzed for cell cycle progression. As compared to hCG controls, FSH stimulated cell cycle progression in the granulosa cells with more numbers of cells in S and G2 phase. In response to the peptide, lesser population of granulosa cells were observed in S phase and subsequent G2/M phase of cell cycle, indicating that cell cycle

progression gets arrested at the preceding G1 to S phase transition (Fig 4; Fig S7). This observation further validates that FSHβ (89-97) peptide can inhibit FSH-FSHR interaction, which is a key mediator of cell growth and cell division in granulosa cells.

Reduction in number of actively multiplying granulosa cells would subsequently lead to arrest in follicular development beyond secondary stage (73)(74). Effect of FSHβ (89-97) peptide on folliculogenesis was evaluated by assessing the ovarian morphology and gene expression analysis. In the immature rats due to low endogenous FSH levels, the ovaries are small and contain a large pool of primordial, primary and secondary follicles (75). In these animals, administration of exogenous FSH facilitates the transition of follicles from secondary to antral stage. Expectedly, the immature rats injected with hCG alone had small ovaries with primordial, primary and secondary follicles and no antral follicles. The treatment with FSH increased the number of growing follicles and multiple antral follicles were observed in the ovaries. When animals were injected with FSHβ (89-97) peptide prior to FSH and hCG injection, higher number of primary and secondary follicles and fewer antral follicles were observed as compared to FSH and hCG treated animals. This experiment revealed that FSHβ (89-97) peptide could inhibit folliculogenesis induced by exogenous FSH. Next, we studied the effect of the peptide on folliculogenesis induced by endogenous circulating FSH using adult female rats. In the adult rats, we studied the effect of FSHβ (89-97) peptide on ovarian, follicular and oocyte morphology. The histopathological observations of ovaries revealed that in both the treatment groups (4 mg/kg BW and 20 mg/kg BW) the number of secondary follicles is higher and antral follicles are fewer as compared to control group (*$p \leq 0.05$ at 20 mg/kg BW; Fig 9A and 9B). Treatment group ovaries also showed large number of empty follicles as compared to control group (Fig 9A and 9B). Comparative and detailed analysis of follicles in treatment and control groups showed that the cumulus granulosa cells morphology is perturbed with presence of pyknotic nuclei in many preantral and antral follicles in treatment group. These observations suggest that FSHβ (89-97) peptide can adversely affect the follicular maturation in the ovaries.

Secretion of reproductive hormones like AMH, inhibins A and B from the gonads are stringently regulated during the course of folliculogenesis. These are considered to be candidate biomarkers of ovarian reserve which are used to measure the follicle number and follicle quality (76)(77). AMH is predominantly secreted by granulosa cells of primary and secondary follicles and is one of the most important regulatory factors in early follicle development (78)(79). Apart from AMH, inhibin A and inhibin B are two other hormones which are heavily dependent on FSH for its secretion (80). Inhibin B is mainly produced by pre-antral or small antral follicles whereas inhibin A is predominantly secreted by large antral or pre-ovulatory follicles (81). The histopathological observations indicate that the follicles in the presence of FSHβ (89-97) peptide are mainly arrested at the pre-antral stage. To further validate the observation, the mRNA levels of AMH, inhibins A and B were evaluated in ovaries of immature rats treated with FSHβ (89-97) peptide (Table1). The ovaries showed elevated mRNA levels of AMH, inhibin B and reduced mRNA levels of inhibin A indicative of arrest in pre-antral phase (Fig 6 A,C and D)(78)(79)(80). The

gene expression analysis reaffirms the fact that folliculogenesis is being affected in response to peptide treatment.

FSH-FSHR interaction in granulosa cells induces CYP19A aromatase expression that aids in conversion of testosterone to estradiol (79). LH-LHR interaction in theca cells leads to testosterone synthesis which in granulosa cells gets aromatized to estradiol under the action of aromatase enzyme (12)(13). Aromatase inhibition in the ovary has shown to reduce serum estradiol levels leading to accumulation of free testosterone in the serum (80). The mRNA levels of aromatase in ovaries of peptide-treated rats were reduced as compared to control animals (Fig 6B). The expression data obtained for aromatase gene was further confirmed by evaluating serum testosterone and estradiol levels in adult female rats. As expected FSHβ (89-97) peptide treated rats showed significantly high testosterone levels and low estradiol levels as compared to control animals (Fig 8F and B). We further evaluated serum progesterone levels in treatment as well as control group. Progesterone synthesis mainly occurs under the influence of LH-LHR interaction in mural and luteinized granulosa cells (12)(13). A recent report has shown that FSH can directly stimulate enzymatic activity of 3β-HSD and triggers conversion of pregnenolone to progesterone in human non-luteinized granulosa cells (81). In case of adult female rats, progesterone levels were found to be high in treatment group (4mg/kg BW) which were reduced at higher dose of peptide (20 mg/kg BW) however, at both the doses the progesterone levels were found to be higher as compared to control group (Fig 8C and D). The hormonal profiling results also correlate with the histopathology data of the adult female rats. We observed that in treatment group, follicles with atretic cumulus granulosa cells had absolutely healthy theca cells. Empty follicles present in treatment group also showed unaltered theca cell morphology (Fig 9A). The results obtained from hormonal profiling and histopathology indicate that FSHβ (89-97) peptide binds to FSHR and modulates its activity.

Here we present a 9-mer peptide derived from FSHβ that harbors FSHR antagonistic activity. To the best of our knowledge, this is the shortest peptide that has been validated for FSHR modulatory activity using various *in silico*, *in vitro* and *in vivo* assays. However, the peptide should be further optimized for its use in fertility regulation and targeted drug delivery. Future work would entail modifying the peptide to incorporate pharmacophoric features that can enhance its potency and drug-like properties.

Acknowledgement:

We are grateful to Dr S. D. Mahale, Director, ICMR-NIRRH for the valuable suggestions and support provided for wet-lab validation. We wish to acknowledge Dr. A. Banerjee and Dr. S. Kutteyil for their guidance in *in vitro* experiments; Ms. S. Raut and Mr. S. Lokhande for help in Steelman-Pohley assay and Mr. P. Salunkhe, Mr. A. Tiwari and Ms. S. Bhaye for help with histopathology staining. We also wish to acknowledge Dr. S. Mukherjee, in-charge of Flow Cytometry facility and Ms. G. Shinde and Ms. S. Khavale for their

assistance in flow cytometry experiments. Dr. A. Contini is grateful to Dr. A. Bazzoli for his precious help in mastering the FlexPepDock software.

This work [RA/766/05-2019] was supported by grants from Department of Biotechnology, Government of India [BT/PR11191/BID/7/485/2014] and Indian Council of Medical Research. The award of senior research scholarship to Ms. K. Prabhudesai by the Lady Tata Memorial Trust, India, is gratefully acknowledged.

References:

1. Agrawal G, Dighe RR. Critical involvement of the hinge region of the follicle-stimulating hormone receptor in the activation of the receptor. J Biol Chem 2009;284(5):2636–47.

2. Sanford JC, Batten BE. Endocytosis of follicle-stimulating hormone by ovarian granulosa cells: analysis of hormone processing and receptor dynamics. J Cell Physiol 1989;138(1):154–64.

3. Fletcher PW, Reichert LEJ. Cellular processing of follicle-stimulating hormone by Sertoli cells in serum-free culture. Mol Cell Endocrinol 1984;34(1):39–49.

4. Bukovsky A, Chen TT, Wimalasena J, Caudle MR. Cellular localization of luteinizing hormone receptor immunoreactivity in the ovaries of immature, gonadotropin-primed and normal cycling rats. Biol Reprod 1993;48(6):1367–82.

5. Zhang FP, Hamalainen T, Kaipia A, Pakarinen P, Huhtaniemi I. Ontogeny of luteinizing hormone receptor gene expression in the rat testis. Endocrinology 1994;134(5):2206–13.

6. Yung Y, Aviel-Ronen S, Maman E, Rubinstein N, Avivi C, Orvieto R, et al. Localization of luteinizing hormone receptor protein in the human ovary. Mol Hum Reprod 2014;20(9):844–9.

7. Jeppesen JV, Kristensen SG, Nielsen ME, Humaidan P, Dal Canto M, Fadini R, et al. LH-receptor gene expression in human granulosa and cumulus cells from antral and preovulatory follicles. J Clin Endocrinol Metab 2012;97(8):E1524-31.

8. Maman E, Yung Y, Kedem A, Yerushalmi GM, Konopnicki S, Cohen B, et al. High expression of luteinizing hormone receptors messenger RNA by human cumulus granulosa cells is in correlation with decreased fertilization. Fertil Steril 2012;97(3):592–8.

9. Gloaguen P, Crepieux P, Heitzler D, Poupon A, Reiter E. Mapping the follicle-stimulating hormone-induced signaling networks. Front Endocrinol (Lausanne) 2011;2:45.

10. Reiter E, Lefkowitz RJ. GRKs and beta-arrestins: roles in receptor silencing, trafficking and signaling. Trends Endocrinol Metab 2006;17(4):159–65.

11. Robker RL, Richards JS. Hormonal control of the cell cycle in ovarian cells: proliferation versus differentiation. Biol Reprod 1998;59(3):476–82.

12. Orisaka M, Tajima K, Tsang BK, Kotsuji F. Oocyte-granulosa-theca cell interactions during preantral follicular development. J Ovarian Res 2009;2(1):9.

13. Kobayashi M, Nakano R, Ooshima A. Immunohistochemical localization of pituitary gonadotrophins and gonadal steroids confirms the “two-cell, two-gonadotrophin” hypothesis of steroidogenesis in the human ovary. J Endocrinol 1990;126(3):483–8.

14. Magoffin DA. Ovarian enzyme activities in women with polycystic ovary syndrome. Fertil Steril 2006;86 Suppl 1:S9–11.

15. Dewailly D, Robin G, Peigne M, Decanter C, Pigny P, Catteau-Jonard S. Interactions between androgens, FSH, anti-Mullerian hormone and estradiol during folliculogenesis in the human normal and polycystic ovary. Hum Reprod Update 2016;22(6):709–24.

16. Karlsson AB, Maizels ET, Flynn MP, Jones JC, Shelden EA, Bamburg JR, et al. Luteinizing hormone receptor-stimulated progesterone production by preovulatory granulosa cells requires protein kinase A-dependent activation/dephosphorylation of the actin dynamizing protein cofilin. Mol Endocrinol 2010;24(9):1765–81.

17. Lamb JD, Shen S, McCulloch C, Jalalian L, Cedars MI, Rosen MP. Follicle-stimulating hormone administered at the time of human chorionic gonadotropin trigger improves oocyte developmental competence in in vitro fertilization cycles: a randomized, double-blind, placebo-controlled trial. Fertil Steril [Internet] 2011 [cited 2019 May 10];95(5):1655–60. Available from: https://linkinghub.elsevier.com/retrieve/pii/S001502821100029X

18. Nataraja SG, Yu HN, Palmer SS. Discovery and Development of Small Molecule Allosteric Modulators of Glycoprotein Hormone Receptors. Front Endocrinol (Lausanne) 2015;6:142.

19. Layman LC. Mutations in the follicle-stimulating hormone-beta (FSH beta) and FSH receptor genes in mice and humans. Semin Reprod Med 2000;18(1):5–10.

20. Abel MH, Wootton AN, Wilkins V, Huhtaniemi I, Knight PG, Charlton HM. The effect of a null mutation in the follicle-stimulating hormone receptor gene on mouse reproduction. Endocrinology 2000;141(5):1795–803.

21. Dierich A, Sairam MR, Monaco L, Fimia GM, Gansmuller A, LeMeur M, et al. Impairing follicle-stimulating hormone (FSH) signaling in vivo: targeted disruption of the FSH receptor leads to aberrant gametogenesis and hormonal imbalance. Proc Natl Acad Sci U S A 1998;95(23):13612–7.

22. Kumar TR, Wang Y, Lu N, Matzuk MM. Follicle stimulating hormone is required for ovarian follicle maturation but not male fertility. Nat Genet 1997;15(2):201–4.

23. Chrusciel M, Ponikwicka-Tyszko D, Wolczynski S, Huhtaniemi I, Rahman NA. Extragonadal FSHR Expression and Function-Is It Real? Front Endocrinol (Lausanne) 2019;10:32.

24. Gartrell BA, Tsao C, Galsky MD. The follicle-stimulating hormone receptor: a novel target in genitourinary malignancies. Urol Oncol 2013;31(8):1403–7.

25. Perales-Puchalt A, Svoronos N, Rutkowski MR, Allegrezza MJ, Tesone AJ, Payne KK, et al. Follicle-Stimulating Hormone Receptor Is Expressed by Most Ovarian Cancer Subtypes and Is a Safe and Effective Immunotherapeutic Target. Clin Cancer Res 2017;23(2):441–53.

26. Zhang X, Chen J, Kang Y, Hong S, Zheng Y, Sun H, et al. Targeted paclitaxel nanoparticles modified with follicle-stimulating hormone beta 81-95 peptide show effective antitumor activity against ovarian carcinoma. Int J Pharm 2013;453(2):498–505.

27. Dragoman M V, Tepper NK, Fu R, Curtis KM, Chou R, Gaffield ME. A systematic review and meta-analysis of venous thrombosis risk among users of combined oral contraception. Int J Gynaecol Obstet 2018;141(3):287–94.

28. Morch LS, Skovlund CW, Hannaford PC, Iversen L, Fielding S, Lidegaard O. Contemporary Hormonal Contraception and the Risk of Breast Cancer. N Engl J Med 2017;377(23):2228–39.

29. Sitruk-Ware R, Nath A. Characteristics and metabolic effects of estrogen and progestins contained in oral contraceptive pills. Best Pract Res Clin Endocrinol Metab 2013;27(1):13–24.

30. Yu HN, Richardson TE, Nataraja S, Fischer DJ, Sriraman V, Jiang X, et al. Discovery of substituted benzamides as follicle stimulating hormone receptor allosteric modulators. Bioorg Med Chem Lett 2014;24(9):2168–72.

31. van Koppen CJ, Verbost PM, van de Lagemaat R, Karstens W-JF, Loozen HJJ, van Achterberg TAE, et al. Signaling of an allosteric, nanomolar potent, low molecular weight agonist for the follicle-stimulating hormone receptor. Biochem Pharmacol 2013;85(8):1162–70.

32. Anderson RC, Newton CL, Millar RP. Small Molecule Follicle-Stimulating Hormone Receptor Agonists and Antagonists. Front Endocrinol (Lausanne) 2018;9:757.

33. Brigger I, Dubernet C, Couvreur P. Nanoparticles in cancer therapy and diagnosis. Adv Drug Deliv Rev 2002;54(5):631–51.

34. Zhang Z, Jia L, Feng Y, Zheng W. Overexpression of follicle-stimulating hormone receptor facilitates the development of ovarian epithelial cancer. Cancer Lett 2009;278(1):56–64.

35. Xu Y, Pan D, Zhu C, Xu Q, Wang L, Chen F, et al. Pilot study of a novel (18)F-

labeled FSHR probe for tumor imaging. Mol imaging Biol MIB Off Publ Acad Mol Imaging 2014;16(4):578–85.

36. Sonawani A, Niazi S, Idicula-Thomas S. Correction: In Silico Study on Binding Specificity of Gonadotropins and Their Receptors: Design of a Novel and Selective Peptidomimetic for Human Follicle Stimulating Hormone Receptor. PLoS One 2013;8(11).

37. Jiang X, Liu H, Chen X, Chen P-H, Fischer D, Sriraman V, et al. Structure of follicle-stimulating hormone in complex with the entire ectodomain of its receptor. Proc Natl Acad Sci U S A 2012;109(31):12491–6.

38. Jorgensen WL, Chandrasekhar J, Madura JD, Impey RW, Klein ML. Comparison of simple potential functions for simulating liquid water. J Chem Phys 1983;79(2):926–35.

39. Le Grand S, Götz AW, Walker RC. SPFP: Speed without compromise - A mixed precision model for GPU accelerated molecular dynamics simulations. Comput Phys Commun 2013;184(2):374–80.

40. Case DA. Amber 18. Univ California, San Fr [Internet] 2018;Available from: http://ambermd.org/doc12/Amber18.pdf

41. Maffucci I, Hu X, Fumagalli V, Contini A. An Efficient Implementation of the Nwat-MMGBSA Method to Rescore Docking Results in Medium-Throughput Virtual Screenings. Front Chem 2018;6:43.

42. Raveh B, London N, Schueler-Furman O. Sub-angstrom modeling of complexes between flexible peptides and globular proteins. Proteins 2010;78(9):2029–40.

43. Leaver-Fay A, Tyka M, Lewis SM, Lange OF, Thompson J, Jacak R, et al. ROSETTA3: an object-oriented software suite for the simulation and design of macromolecules. Methods Enzymol 2011;487:545–74.

44. Raveh B, London N, Zimmerman L, Schueler-Furman O. Rosetta FlexPepDock ab-initio: simultaneous folding, docking and refinement of peptides onto their receptors. PLoS One 2011;6(4):e18934.

45. Jones DT. Protein secondary structure prediction based on position-specific scoring matrices. J Mol Biol 1999;292(2):195–202.

46. Weng G, Wang E, Chen F, Sun H, Wang Z, Hou T. Assessing the performance of MM/PBSA and MM/GBSA methods. 9. Prediction reliability of binding affinities and binding poses for protein-peptide complexes. Phys Chem Chem Phys 2019;21(19):10135–45.

47. Maier JA, Martinez C, Kasavajhala K, Wickstrom L, Hauser KE, Simmerling C. ff14SB: Improving the Accuracy of Protein Side Chain and Backbone Parameters from ff99SB. J Chem Theory Comput 2015;11(8):3696–713.

48. Nguyen H, Roe DR, Simmerling C. Improved Generalized Born Solvent Model Parameters for Protein Simulations. J Chem Theory Comput 2013;9(4):2020–34.

49. Hu X, Contini A. Rescoring Virtual Screening Results with the MM-PBSA Methods: Beware of Internal Dielectric Constants. J Chem Inf Model 2019;59(6):2714–28.

50. Maffucci I, Contini A. Improved Computation of Protein-Protein Relative Binding Energies with the Nwat-MMGBSA Method. J Chem Inf Model 2016;56(9):1692–704.

51. Maffucci I, Contini A. Explicit Ligand Hydration Shells Improve the Correlation between MM-PB/GBSA Binding Energies and Experimental Activities. J Chem Theory Comput 2013;9(6):2706–17.

52. Massova I, Kollman PA. Combined molecular mechanical and continuum solvent approach (MM-PBSA/GBSA) to predict ligand binding. Perspect Drug Discov Des [Internet] 2000;18(1):113–35. Available from: https://doi.org/10.1023/A:1008763014207

53. Miller BR 3rd, McGee TDJ, Swails JM, Homeyer N, Gohlke H, Roitberg AE. MMPBSA.py: An Efficient Program for End-State Free Energy Calculations. J Chem Theory Comput 2012;8(9):3314–21.

54. Kene PS, Nalavadi VC, Dighe RR, Iyer KS, Mahale SD. Identification of the structural and functional determinants of the extracellular domain of the human follicle stimulating hormone receptor. J Endocrinol 2004;182(3):501–8.

55. Fraker PJ, Speck JCJ. Protein and cell membrane iodinations with a sparingly soluble chloroamide, 1,3,4,6-tetrachloro-3a,6a-diphrenylglycoluril. Biochem Biophys Res Commun 1978;80(4):849–57.

56. Dupakuntla M, Pathak B, Roy BS, Mahale SD. Extracellular loop 2 in the FSH receptor is crucial for ligand mediated receptor activation. Mol Cell Endocrinol 2012;362(1–2):60–8.

57. STEELMAN SL, POHLEY FM. Assay of the follicle stimulating hormone based on the augmentation with human chorionic gonadotropin. Endocrinology 1953;53(6):604–16.

58. Dias JA, Bonnet B, Weaver BA, Watts J, Kluetzman K, Thomas RM, et al. A negative allosteric modulator demonstrates biased antagonism of the follicle stimulating hormone receptor. Mol Cell Endocrinol 2011;333(2):143–50.

59. Grasso P, Rozhavskaya M, Reichert LEJ. In vivo effects of human follicle-stimulating hormone-related synthetic peptide hFSH-beta-(81-95) and its subdomain hFSH-beta-(90-95) on the mouse estrous cycle. Biol Reprod 1998;58(3):821–5.

60. Chitnis SS, Navlakhe RM, Shinde GC, Barve SJ, D'Souza S, Mahale SD, et al.

Granulosa cell apoptosis induced by a novel FSH binding inhibitory peptide from human ovarian follicular fluid. J Histochem Cytochem 2008;56(11):961–8.

61. Godbole G, Suman P, Malik A, Galvankar M, Joshi N, Fazleabas A, et al. Decrease in Expression of HOXA10 in the Decidua After Embryo Implantation Promotes Trophoblast Invasion. Endocrinology 2017;158(8):2618–33.

62. Desai SS, Achrekar SK, Pathak BR, Desai SK, Mangoli VS, Mangoli R V, et al. Follicle-stimulating hormone receptor polymorphism (G-29A) is associated with altered level of receptor expression in Granulosa cells. J Clin Endocrinol Metab 2011;96(9):2805–12.

63. Sahu B, Shah S, Prabhudesai K, Contini A, Idicula-Thomas S. Discovery of small molecule binders of human FSHR(TMD) with novel structural scaffolds by integrating structural bioinformatics and machine learning algorithms. J Mol Graph Model 2019;89:156–66.

64. Aldeghi M, Bodkin MJ, Knapp S, Biggin PC. Statistical Analysis on the Performance of Molecular Mechanics Poisson-Boltzmann Surface Area versus Absolute Binding Free Energy Calculations: Bromodomains as a Case Study. J Chem Inf Model 2017;57(9):2203–21.

65. Fan QR, Hendrickson WA. Structure of human follicle-stimulating hormone in complex with its receptor. Nature 2005;433(7023):269–77.

66. Campbell RK, Dean-Emig DM, Moyle WR. Conversion of human choriogonadotropin into a follitropin by protein engineering. Proc Natl Acad Sci U S A 1991;88(3):760–4.

67. Dias JA, Zhang Y, Liu X. Receptor binding and functional properties of chimeric human follitropin prepared by an exchange between a small hydrophilic intercysteine loop of human follitropin and human lutropin. J Biol Chem 1994;269(41):25289–94.

68. Santa Coloma TA, Reichert LEJ. Identification of a follicle-stimulating hormone receptor-binding region in hFSH-beta-(81-95) using synthetic peptides. J Biol Chem 1990;265(9):5037–42.

69. Christin-Maitre S, Bouchard P. Bioassays of gonadotropins based on cloned receptors. Mol Cell Endocrinol 1996;125(1–2):151–9.

70. Kottler M-L, Chou Y-Y, Chabre O, Richard N, Polge C, Brailly-Tabard S, et al. A new FSHbeta mutation in a 29-year-old woman with primary amenorrhea and isolated FSH deficiency: functional characterization and ovarian response to human recombinant FSH. Eur J Endocrinol 2010;162(3):633–41.

71. Liu H, Xu X, Han T, Yan L, Cheng L, Qin Y, et al. A novel homozygous mutation in the FSHR gene is causative for primary ovarian insufficiency. Fertil Steril 2017;108(6):1050-1055.e2.

72. Achrekar SK, Modi DN, Meherji PK, Patel ZM, Mahale SD. Follicle stimulating hormone receptor gene variants in women with primary and secondary amenorrhea. J Assist Reprod Genet 2010;27(6):317–26.

73. Conway BA, Mahesh VB, Mills TM. Effect of dihydrotestosterone on the growth and function of ovarian follicles in intact immature female rats primed with PMSG. J Reprod Fertil 1990;90(1):267–77.

74. Pradeep PK, Li X, Peegel H, Menon KMJ. Dihydrotestosterone inhibits granulosa cell proliferation by decreasing the cyclin D2 mRNA expression and cell cycle arrest at G1 phase. Endocrinology 2002;143(8):2930–5.

75. Picut CA, Dixon D, Simons ML, Stump DG, Parker GA, Remick AK. Postnatal ovary development in the rat: morphologic study and correlation of morphology to neuroendocrine parameters. Toxicol Pathol 2015;43(3):343–53.

76. Andersen CY, Byskov AG. Estradiol and regulation of anti-Mullerian hormone, inhibin-A, and inhibin-B secretion: analysis of small antral and preovulatory human follicles' fluid. J Clin Endocrinol Metab 2006;91(10):4064–9.

77. Randolph JFJ, Harlow SD, Helmuth ME, Zheng H, McConnell DS. Updated assays for inhibin B and AMH provide evidence for regular episodic secretion of inhibin B but not AMH in the follicular phase of the normal menstrual cycle. Hum Reprod 2014;29(3):592–600.

78. Hayes E, Kushnir V, Ma X, Biswas A, Prizant H, Gleicher N, et al. Intra-cellular mechanism of Anti-Mullerian hormone (AMH) in regulation of follicular development. Mol Cell Endocrinol 2016;433:56–65.

79. Fleming R, Seifer DB, Frattarelli JL, Ruman J. Assessing ovarian response: antral follicle count versus anti-Mullerian hormone. Reprod Biomed Online 2015;31(4):486–96.

80. Kristensen SG, Mamsen LS, Jeppesen J V, Botkjaer JA, Pors SE, Borgbo T, et al. Hallmarks of Human Small Antral Follicle Development: Implications for Regulation of Ovarian Steroidogenesis and Selection of the Dominant Follicle. Front Endocrinol (Lausanne) 2017;8:376.

81. Hohmann FP, Laven JSE, de Jong FH, Fauser BCJM. Relationship between inhibin A and B, estradiol and follicle growth dynamics during ovarian stimulation in normo-ovulatory women. Eur J Endocrinol 2005;152(3):395–401.